



LETTERS TO THE EDITOR



IMPEDANCE MATRIX SYNTHESIS FOR MULTIPLY CONNECTED EXHAUST NETWORK SYSTEMS USING THE DIRECT MIXED-BODY BEM

G. LOU AND T. W. WU

Department of Mechanical Engineering, University of Kentucky, Lexington, KY 40506, U.S.A.

AND

C. Y. R. CHENG

Nelson Industries, Inc. Stoughton, WI 53589, U.S.A.

(Received 11 June 1999, and in final form 8 March 2000)

1. INTRODUCTION

Mufflers and silencers used in industry usually contain very complex internal geometry, such as extended inlet/outlet tubes, thin baffles, and perforated tubes. In a recent paper, Wu and Wan [1] proposed a direct mixed-body boundary element method (BEM) to model mufflers and silencers with thin and perforated internal components. The direct mixed-body BEM eliminates the tedious zoning and interface matching steps in the multi-domain BEM. To evaluate the transmission loss (TL), Wu and Wan [1] also used a so-called “three-point method” [2] as an alternative to the traditional four-pole transfer matrix method [3]. The three-point method requires only one single BEM run at each frequency, while the traditional four-pole method requires two separate BEM runs. However, unlike the four-pole method, the three-point method does not produce the four-pole transfer matrix. The four-pole transfer matrix relates the acoustic variables at the inlet directly to the acoustic variables at the outlet. This important property may allow a very large system to be divided into smaller subsystems in series connection for analysis purposes. Since the three-point method produces only the TL for the entire system, it can not be used for the analysis of any subsystems. This is the major drawback of the three-point method.

From the system point of view, a method that can be applied to subsystems is still preferred because real-world systems are usually too big to fit in one single computer model. Dividing a large system into smaller subsystems for analysis purposes is always preferred. To speed up the conventional four-pole method, Wu *et al.* [4] used an improved method to obtain the four-pole transfer matrix. This improved method simply permutes the variables used in the conventional four-pole transfer matrix in such a way that only one single BEM matrix needs to be solved at each frequency. As a consequence, the improved four-pole method is as fast as the three-point method in evaluating the TL. More importantly, the improved method also produces the four-pole transfer matrix. The permuted four-pole matrix is actually the impedance matrix and it can be easily converted back to the conventional four-pole transfer matrix. It should be noted that such a conversion technique was first proposed by Kim and Soedel [5–7] in a modal expansion method for three-dimensional cavity problems, although the numerical benefit of this conversion was

not recognized then. The same conversion has also been used by Ji *et al.* [8] in evaluating the TL for mufflers with a mean flow.

Even with the improved method to obtain the four-pole parameters, there are still two problems with the four-pole transfer matrix approach. First, the four-pole transfer matrix is only defined for systems (or subsystems) with a single inlet and a single outlet. For systems (or subsystems) with multiple inlets/outlets, the transfer matrix relating the acoustic variables at the inlets to the acoustic variables at the outlets may not be uniquely defined. Second, for subsystems connected in parallel instead of in series, the simple matrix multiplication operation on the transfer matrices is not valid anymore.

Alternative matrix formulations have been suggested by Frid [9], Eversman [10], and Glav and Abom [11]. In particular, Frid [9] used a mobility matrix that relates the acoustic pressure at the inlet and the outlet to the corresponding volume velocities. With the mobility matrix formulation it is possible to easily assemble the mobility matrix for a complicated network system.

In this paper, an approach called impedance matrix synthesis (IMS) is used along with the BEM to evaluate the TL of multiply connected exhaust systems. The impedance matrix is the inverse of the mobility matrix used in reference [9]. Actually, combining the impedance matrices of substructures into a resultant impedance matrix has also been used by Ji *et al.* [8] in the multi-domain BEM analysis. Like the transfer matrix reported earlier by Tanaka *et al.* [12], the impedance matrix in Reference [8] was applied to BEM mesh-dependant substructures to improve the efficiency of the multi-domain BEM. In this paper, the impedance matrix is used in a slightly different way so that the matrix is no longer a BEM mesh-dependent product, but rather a physical property of real subsystems. That means the impedance matrix can even be measured or evaluated without using the BEM.

In references [4, 8], the resultant impedance matrix for a two-port system was eventually converted back to the conventional four-pole transfer matrix for the purpose of evaluating the TL. Now it has become clear to the authors that such a conversion is unnecessary. The TL can be directly evaluated from the resultant impedance matrix itself, regardless of the number of outlets. What is more important is that the impedance matrix is much easier to operate than the four pole transfer matrix for multiply connected network systems. In addition, the impedance matrix approach is ideally suited to the BEM because only one BEM matrix needs to be solved at each frequency, regardless of the number of inlets and outlets in the subsystem under consideration.

Three test cases are given to demonstrate the impedance matrix approach. The first test case is a simple expansion chamber with two outlets. This test case is to demonstrate how to evaluate the TL directly from the impedance matrix. Note that the four-pole transfer matrix is not defined for a system with two outlets. The second test case is a double-expansion chamber with two external interconnecting tubes. This set case is to demonstrate how to use the IMS to combine subsystems with multiple interconnections. The third test case is similar to the second one except that the two interconnecting tubes are internal. All the numerical results are verified by experimental data.

2. DIRECT MIXED-BODY BEM

In this section, the direct mixed-body boundary integral formulation by Wu and Wan [1] is briefly reviewed. With reference to Figure 1, let S_r , S_t , and S_p denote the regular, thin and perforated surfaces respectively. The interior acoustic domain is denoted by Ω . Let \mathbf{n} be the unit normal vector. The unit normal vector on S_r is directing into the interior acoustic

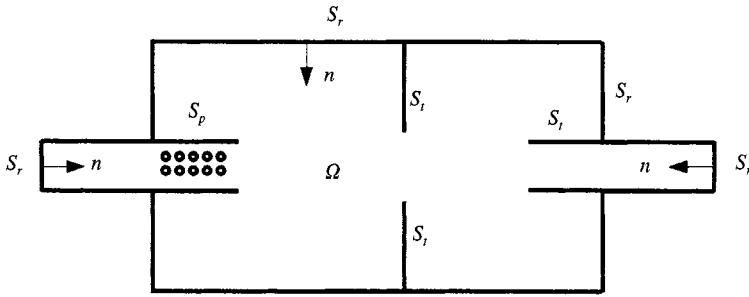


Figure 1. Surface definition used in the direct mixed-body BEM.

domain. The unit normal vector on S_p and S_t can be directing into either side of the thin/perforated surface. The side into which \mathbf{n} is directing is called the positive side.

Let p denote the sound pressure, and v_n denote the normal velocity of the surface. We adopt the $e^{+i\omega t}$ convention in steady state linear acoustics, where $i = \sqrt{-1}$ and ω is the angular frequency. Assume the thin surfaces are rigid, and the direct mixed-body boundary integral equations are [1, 4]

$$\int_{S_t+S_p} \frac{\partial \Psi}{\partial n} (p^+ - p^-) dS + \int_{S_p} \left(p \frac{\partial \Psi}{\partial n} + i\rho\omega v_n \psi \right) dS$$

$$= \begin{cases} 4\pi p(P), & P \in \Omega, \\ 2\pi p(P), & P \in S_r, \\ 2\pi [p^+(P) + p^-(P)], & P \in S_t + S_p, \end{cases} \quad (1a)$$

$$= \begin{cases} 4\pi p(P), & P \in \Omega, \\ 2\pi p(P), & P \in S_r, \\ 2\pi [p^+(P) + p^-(P)], & P \in S_t + S_p, \end{cases} \quad (1b)$$

$$= \begin{cases} 4\pi p(P), & P \in \Omega, \\ 2\pi p(P), & P \in S_r, \\ 2\pi [p^+(P) + p^-(P)], & P \in S_t + S_p, \end{cases} \quad (1c)$$

$$\int_{S_t+S_p} \frac{\partial^2 \Psi}{\partial n \partial n^p} (p^+ - p^-) dS + \int_{S_p} \left(p \frac{\partial^2 \Psi}{\partial n \partial n^p} + i\rho\omega v_n \frac{\partial \psi}{\partial n^p} \right) dS$$

$$= \begin{cases} -4\pi i\rho\omega v_n(P), & P \in S_t, \\ 4\pi \frac{ik}{\xi} [p^+(P) - p^-(P)], & P \in S_p, \end{cases} \quad (2a)$$

$$= \begin{cases} -4\pi i\rho\omega v_n(P), & P \in S_t, \\ 4\pi \frac{ik}{\xi} [p^+(P) - p^-(P)], & P \in S_p, \end{cases} \quad (2b)$$

where P is the collocation point, ψ is the free-space Green's function, ρ is the mean density of the fluid, k is the wavenumber, and ξ is the non-dimensional transfer impedance [13] for the perforated surface S_p . In the above equations, p^+ is the sound pressure on the positive side of S_t or S_p , and p^- is the sound pressure on the opposite side. The explicit expression for ψ is

$$\psi = \frac{e^{-ikr}}{r}, \quad (3)$$

where $r = |P - Q|$, and Q is any integration point on the boundary. In equation (2), $\partial/\partial n^p$ means partial differentiation with respect to the coordinates of P in the normal direction of P . Equations (1b), (2a), and (2b) are solved simultaneously for pressure on S_r , and pressure jump on S_t and S_p .

3. IMPEDANCE MATRIX SYNTHESIS

As shown in Figure 2, a simple network system that consists of a Y-shaped distributor and two interconnected silencers is used as an example to demonstrate the impedance

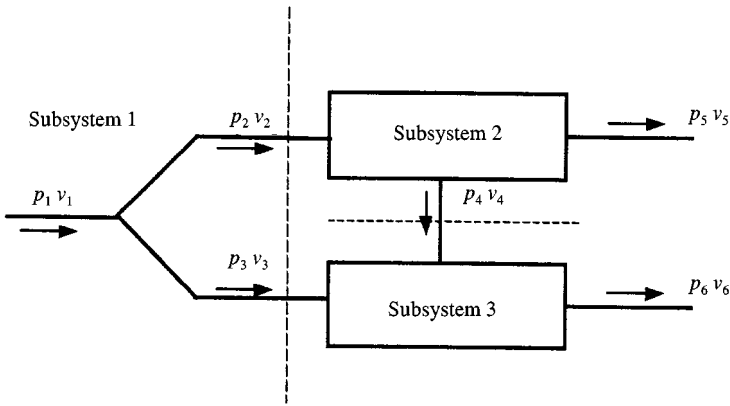


Figure 2. A simple network system.

matrix synthesis. The network system is divided into three subsystems by the two imaginary cuts (dotted lines) as shown in the figure. All the cuts are made at connecting tubes where the acoustic variables are assumed constant over the tube cross-section. The sound pressure and the particle velocity at the inlet are denoted by p_1 and v_1 respectively. At the two outlets, $p_5 v_5$, p_6 and v_6 are the corresponding acoustic variables. The variables at the cuts, p_2 , v_2 , p_3 , v_3 , p_4 , and v_4 , are referred to as the internal variables. The directions of the velocities are defined by the arrows shown in the figure. It is noted that the four-pole transfer matrix is not defined for the entire system or any of the three subsystems.

Without the four-pole transfer matrix, one can still define an impedance matrix for each subsystem as follows.

For subsystem 1 (Y-shaped distributor, one inlet and two outlets):

$$\begin{bmatrix} p_1 \\ p_2 \\ p_3 \end{bmatrix} = \begin{bmatrix} a_{11} & a_{12} & a_{13} \\ a_{21} & a_{22} & a_{23} \\ a_{31} & a_{32} & a_{33} \end{bmatrix} \begin{bmatrix} v_1 \\ v_2 \\ v_3 \end{bmatrix}. \quad (4)$$

For subsystem 2 (upper silencer, one inlet and two outlets),

$$\begin{bmatrix} p_2 \\ p_4 \\ p_5 \end{bmatrix} = \begin{bmatrix} b_{11} & b_{12} & b_{13} \\ b_{21} & b_{22} & b_{23} \\ b_{31} & b_{32} & b_{33} \end{bmatrix} \begin{bmatrix} v_2 \\ v_4 \\ v_5 \end{bmatrix}. \quad (5)$$

For subsystem 3 (lower silencer, two inlets and one outlet),

$$\begin{bmatrix} p_3 \\ p_4 \\ p_6 \end{bmatrix} = \begin{bmatrix} c_{11} & c_{12} & c_{13} \\ c_{21} & c_{22} & c_{23} \\ c_{31} & c_{32} & c_{33} \end{bmatrix} \begin{bmatrix} v_3 \\ v_4 \\ v_6 \end{bmatrix}. \quad (6)$$

Each column of the impedance matrix can be obtained by a BEM run with an appropriate set of velocity boundary conditions at the inlets and outlets. For example, column one of equation (4) is obtained by setting $v_1 = 1$ and $v_2 = v_3 = 0$ in the BEM model of subsystem 1. Similarly, column 2 of equation (4) is obtained by setting $v_2 = 1$ and $v_1 = v_3 = 0$ in the

BEM model, and column 3 by setting $v_3 = 1$ and $v_1 = v_2 = 0$. According to the reciprocal theorem [14], if there is no bulk-reacting material or sound source inside the system, the off-diagonal terms of the impedance matrix should be either symmetric or antisymmetric, depending on the definition of velocity direction (in or out). For example, $a_{12} = -a_{21}$ and $a_{13} = -a_{31}$ because v_1 is in while v_2 and v_3 are out. On the other hand, $a_{23} = a_{32}$ because both v_1 and v_2 are out.

It is noticed that three different BEM runs are needed to obtain the complete impedance matrix of each subsystem. Nevertheless, for each subsystem, only one BEM matrix needs to be decomposed at each frequency, because the three BEM runs share the same BEM coefficient matrix. The second and third BEM runs use only a different velocity condition than the first BEM run, and therefore, require only a trivial back-substitution procedure. Actually, the three BEM runs can be done simultaneously because the three right-hand side vectors corresponding to the three different sets of velocity boundary conditions may be formed at the same time.

With the three subsystem impedance matrices ready, the next step is to combine the matrices into a resultant impedance matrix for the combined system. To begin with, the resultant impedance matrix is defined by

$$\begin{bmatrix} p_1 \\ p_5 \\ p_6 \end{bmatrix} = \begin{bmatrix} z_{11} & z_{12} & z_{13} \\ z_{21} & z_{22} & z_{23} \\ z_{31} & z_{32} & z_{33} \end{bmatrix} \begin{bmatrix} v_1 \\ v_5 \\ v_6 \end{bmatrix}. \quad (7)$$

It is clear that three different boundary-value problems need to be solved in order to determine the resultant impedance matrix. Without calling the BEM again, one can synthesize the existing impedance matrices for the subsystems to obtain the impedance matrix for the combined system. With $v_1, v_5,$ and v_6 specified, the unknowns are $p_1, p_5, p_6,$ and the six internal variables ($p_2, v_2, p_3, v_3, p_4, v_4$), a total of nine. Notice that equations (4–6) provide a total of nine equations for the nine unknowns. Assemble equations (4–6) into a global 9×9 matrix equation. That is,

$$\begin{bmatrix} 1 & 0 & 0 & 0 & 0 & 0 & -a_{12} & -a_{13} & 0 \\ 0 & 1 & 0 & 0 & 0 & 0 & -a_{22} & -a_{23} & 0 \\ 0 & 0 & 1 & 0 & 0 & 0 & -a_{32} & -a_{33} & 0 \\ 0 & 1 & 0 & 0 & 0 & 0 & -b_{11} & 0 & -b_{12} \\ 0 & 0 & 0 & 1 & 0 & 0 & -b_{21} & 0 & -b_{22} \\ 0 & 0 & 0 & 0 & 1 & 0 & -b_{31} & 0 & -b_{32} \\ 0 & 0 & 1 & 0 & 0 & 0 & 0 & -c_{11} & -c_{12} \\ 0 & 0 & 0 & 1 & 0 & 0 & 0 & -c_{21} & -c_{22} \\ 0 & 0 & 0 & 0 & 0 & 1 & 0 & -c_{31} & -c_{32} \end{bmatrix} \begin{bmatrix} p_1 \\ p_2 \\ p_3 \\ p_4 \\ p_5 \\ p_6 \\ v_2 \\ v_3 \\ v_4 \end{bmatrix} = \begin{bmatrix} a_{11}v_1 \\ a_{21}v_1 \\ a_{31}v_1 \\ b_{13}v_5 \\ b_{23}v_5 \\ b_{33}v_5 \\ c_{13}v_6 \\ c_{23}v_6 \\ c_{33}v_6 \end{bmatrix} \quad (8)$$

Solve the above 9×9 matrix equation three times. For the first time, the boundary conditions are $v_1 = 1, v_5 = 0$ and $v_6 = 0$. For the second time, $v_1 = 0, v_5 = 1$ and $v_6 = 0$, and for the third time $v_1 = 0, v_5 = 0$ and $v_6 = 1$. Each time pick up $p_1, p_5,$ and p_6 from the solution vector, and the impedance matrix components are thus obtained. Use the reciprocal theorem, if applicable, to check the symmetry or antisymmetry of the off-diagonal terms. For this example problem, $z_{12} = -z_{21}, z_{13} = -z_{31}$ and $z_{23} = z_{32}$.

4. TRANSMISSION LOSS

The TL can be directly evaluated from the resultant impedance matrix. Two configurations are considered in this section to demonstrate the procedure. The first configuration has one single inlet and one single outlet. The second configuration has one inlet and two outlets.

4.1. TL FOR SYSTEMS WITH ONE INLET AND ONE OUTLET

For a two-port system with one inlet and one outlet, the TL can be easily obtained by the traditional four-pole transfer matrix. Here we just demonstrate an alternative way to evaluate the TL directly from the impedance matrix. For a two-port system, the impedance matrix is defined by

$$\begin{bmatrix} p_1 \\ p_2 \end{bmatrix} = \begin{bmatrix} z_{11} & z_{12} \\ z_{21} & z_{22} \end{bmatrix} \begin{bmatrix} v_1 \\ v_2 \end{bmatrix}, \quad (9)$$

where subscript 1 refers to the inlet, and 2 refers to the outlet. The sound pressure p at any point inside the inlet tube is composed of an incident wave p_i and a reflected wave p_r . That is,

$$p = p_i + p_r = P_i e^{-ikx} + P_r e^{ikx}, \quad (10)$$

where P_i and P_r are the complex amplitudes of the incident and reflected waves, respectively, and x is the positive axial direction along the tube. The velocity v in the x direction is obtained from the momentum equation

$$v = -\frac{1}{i\rho\omega} \frac{\partial p}{\partial x}. \quad (11)$$

Carry out the differentiation and it can be shown that at any point inside the tube

$$v = \frac{P_i - P_r}{\rho c}. \quad (12)$$

Assume anechoic termination at the outlet end. Then there is only one outgoing wave (or transmitted wave) p_t in the outlet tube, and the velocity in the outlet tube is simply $v = p_t/\rho c$.

Apply the above equations to the inlet and the outlet positions, noting that the fluid density and the speed of sound may change values due to possible temperature gradient. Hence,

$$p_1 = p_i + p_r, \quad v_1 = \frac{P_i - P_r}{\rho_1 c_1}, \quad (13, 14)$$

$$p_2 = p_t, \quad v_2 = \frac{P_t}{\rho_2 c_2}. \quad (15, 16)$$

Substituting equations (13)–(16) into the impedance matrix equation, equation (9) becomes

$$p_i + p_r = z_{11} \frac{P_i - P_r}{\rho_1 c_1} + z_{12} \frac{P_t}{\rho_2 c_2}, \quad (17)$$

$$p_t = z_{21} \frac{P_i - P_r}{\rho_1 c_1} + z_{22} \frac{P_t}{\rho_2 c_2}. \quad (18)$$

Solve equation (17) and (18) for p_i and p_r in terms of p_t . Then find the ratio between p_i and p_t :

$$\frac{p_i}{p_t} = \frac{1}{2} \left[-\frac{z_{11} + \rho_1 c_1}{z_{21}} \left(\frac{z_{22}}{\rho_2 c_2} - 1 \right) + \frac{z_{12}}{\rho_2 c_2} \right]. \quad (19)$$

Finally, the TL can be evaluated by

$$TL = 10 \log \frac{W_i}{W_t} = 20 \log \left| \frac{p_i}{p_t} \right| + 10 \log \frac{\rho_2 c_2}{\rho_1 c_1} + 10 \log \frac{S_1}{S_2}, \quad (20)$$

where W denotes the power, and S_1 and S_2 are the cross-sectional areas of the inlet and outlet tubes respectively.

4.2. TL FOR SYSTEMS WITH ONE INLET AND TWO OUTLETS

For systems with one inlet and two outlets, the impedance matrix is defined by

$$\begin{bmatrix} p_1 \\ p_2 \\ p_3 \end{bmatrix} = \begin{bmatrix} z_{11} & z_{12} & z_{13} \\ z_{21} & z_{22} & z_{23} \\ z_{31} & z_{32} & z_{33} \end{bmatrix} \begin{bmatrix} v_1 \\ v_2 \\ v_3 \end{bmatrix}, \quad (21)$$

where subscript 1 refers to the inlet, and 2 and 3 refer to the two outlets. Assume anechoic termination at both outlet ends. Let p_{t1} denote the transmitted wave in the first outlet tube, and p_{t2} denote the transmitted wave in the second outlet tube. Follow the same procedure as in the one-outlet case. Equation (21) becomes

$$p_i + p_r = z_{11} \frac{p_i - p_r}{\rho_1 c_1} + z_{12} \frac{p_{t1}}{\rho_2 c_2} + z_{13} \frac{p_{t2}}{\rho_3 c_3}, \quad (22)$$

$$p_{t1} = z_{21} \frac{p_i - p_r}{\rho_1 c_1} + z_{22} \frac{p_{t1}}{\rho_2 c_2} + z_{23} \frac{p_{t2}}{\rho_3 c_3}, \quad (23)$$

$$p_{t2} = z_{31} \frac{p_i - p_r}{\rho_1 c_1} + z_{32} \frac{p_{t1}}{\rho_2 c_2} + z_{33} \frac{p_{t2}}{\rho_3 c_3}. \quad (24)$$

First eliminate $p_i - p_r$ from equations (23) and (24); then, p_{t1} is related to p_{t2} by a factor e_3 :

$$p_{t1} = e_3 p_{t2} = \frac{z_{21} + e_2 / (\rho_3 c_3)}{z_{31} - e_1 / (\rho_2 c_2)} p_{t2}, \quad (25)$$

where

$$e_1 = z_{22} z_{31} - z_{32} z_{21}, \quad e_2 = z_{23} z_{31} - z_{33} z_{21}. \quad (26, 27)$$

Substitute this relationship into equations (22) and (23) to solve for p_i and p_r in terms of p_{t2} . Then the ratio between p_i and p_{t2} is

$$\frac{p_i}{p_{t2}} = \frac{\rho_1 c_1}{2 z_{21}} \left[\frac{z_{21}}{\rho_1 c_1} f_1 - \left(1 + \frac{z_{11}}{\rho_1 c_1} \right) f_2 \right], \quad (28)$$

where

$$f_1 = \frac{z_{12}}{\rho_2 c_2} e_3 + \frac{z_{13}}{\rho_3 c_3}, \quad f_2 = \left(\frac{z_{22}}{\rho_2 c_2} - 1 \right) e_3 + \frac{z_{23}}{\rho_3 c_3}. \quad (29, 30)$$

Finally, the TL is evaluated by

$$\begin{aligned} TL &= 10 \log \frac{W_i}{W_{i1} + W_{i2}} = 10 \log \frac{(p_i^2 / \rho_1 c_1) S_1}{(p_{i1}^2 / \rho_2 c_2) S_2 + (p_{i2}^2 / \rho_3 c_3) S_3} \\ &= 10 \log \frac{(p_i^2 / \rho_1 c_1) S_1}{((e_3^2 / \rho_2 c_2) S_2 + (1 / \rho_3 c_3) S_3) p_{i2}^2} \\ &= 20 \log \left| \frac{p_i}{p_{i2}} \right| + 10 \log \frac{(1 / \rho_1 c_1) S_1}{(e_3^2 / \rho_2 c_2) S_2 + (1 / \rho_3 c_3) S_3}, \end{aligned} \quad (31)$$

where S_1 , S_2 , and S_3 are cross-sectional areas of the inlet and outlets, and the pressure ratio is evaluated by equation (28).

5. TEST CASES

Three test cases are presented in this section to demonstrate the IMS approach. The first test case is a simple expansion chamber with one inlet and two outlets. The geometry of the expansion chamber is given in Figure 3. Since this test case has only one system, there is no synthesis involved. The impedance matrix of the chamber is evaluated by the BEM and the TL is evaluated by equation (31). Figure 4 shows the comparison between the TL curve evaluated by the impedance matrix approach and the experimental TL data. It can be seen that the numerical result compares fairly well with the experimental data.

The second test case is a double expansion chamber with two interconnecting tubes. The geometry of the problem is showed in Figure 5. To apply the IMS, the system is cut into two subsystems along the dotted line (A–A). The first subsystem has one inlet and two outlets. The second subsystem has two inlets and one outlet. The impedance matrix for each subsystem is obtained separately by the BEM. Then the IMS is applied to combine the matrices into a resultant impedance matrix for the whole system. The TL is evaluated by equation (20). Figure 6 shows the comparison between the IMS result and the experimental data. Again, very good agreement is observed.

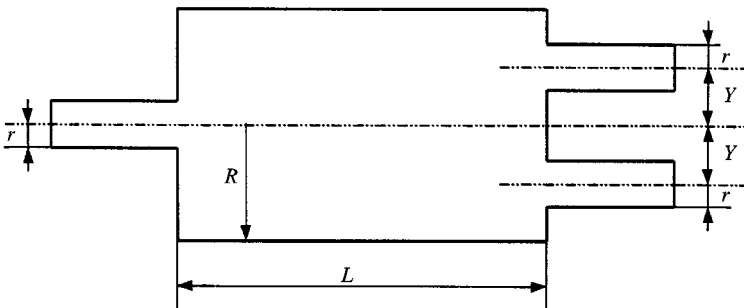


Figure 3. Geometry of the first test case, $R = 0.1016$ m, $r = 0.0254$ m, $Y = 0.0508$ m, $L = 0.4572$ m.

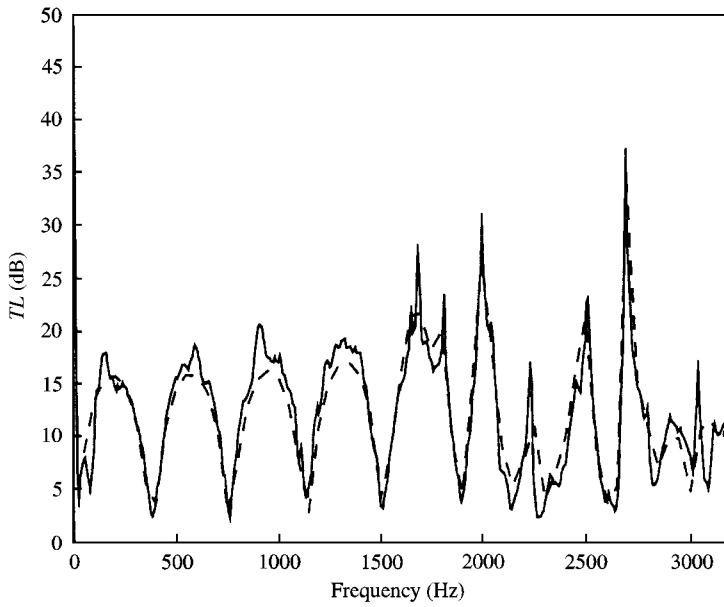


Figure 4. Comparison between the numerical result (---) and the experimental data (—) for the first test case.

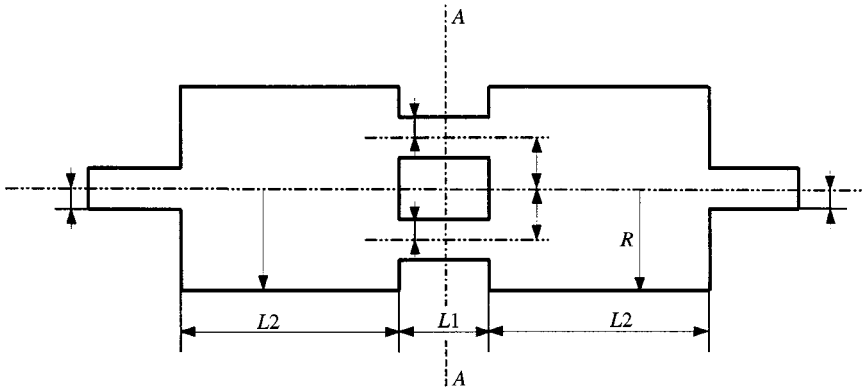


Figure 5. Geometry of the second test case, $R = 0.1016$ m, $r = 0.0241$ m, $Y = 0.0508$ m, $L1 = 0.1524$ m, $L2 = 0.3048$ m.

The third test case is similar to the second test case except that the two interconnecting tubes are internal. The geometry of the problem is shown in Figure 7. A cut along the dotted line A-A is made to divide the system into two subsystems. Each subsystem still contains some thin surfaces due to the extended tubes. The comparison between the IMS result and the experimental data is shown in Figure 8. Very good comparison is observed.

6. CONCLUSIONS

The impedance matrix is used to replace the conventional four-pole transfer matrix for the BEM analysis of mufflers and silencers. The impedance matrix provides more flexibility

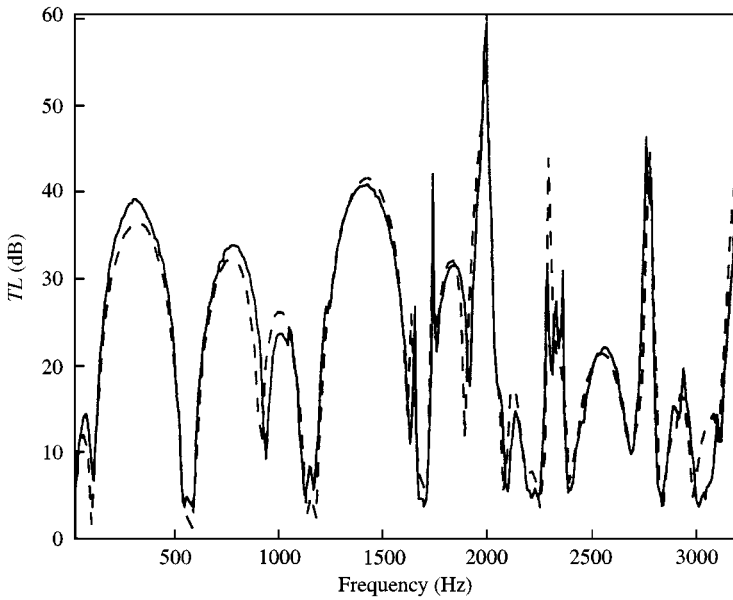


Figure 6. Comparison between the numerical result (---) and the experimental data (—) for the second test case.

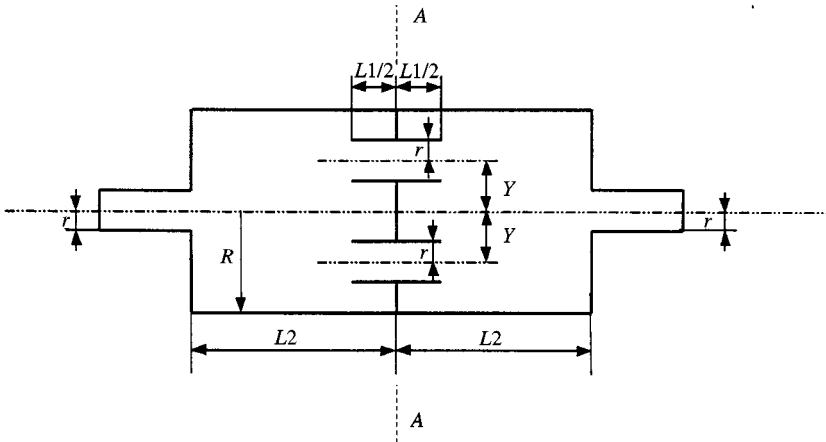


Figure 7. Geometry of the third test case, $R = 0.1016$ m, $r = 0.0241$ m, $Y = 0.0508$ m, $L1 = 0.1524$ m, $L2 = 0.3048$ m.

in combining subsystems into a multiply connected network system. The approach is very efficient because for each subsystem only one BEM matrix needs to be solved at each frequency.

The TL can be directly evaluated from the resultant impedance matrix, regardless of the number of outlets. Formulas for evaluating the TL are derived. Three test cases are studied and numerical results have shown very good agreement with experimental data.

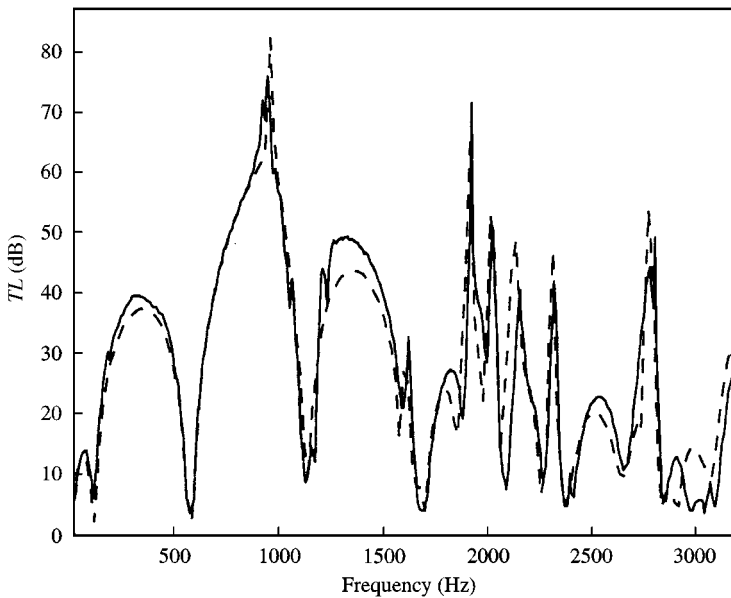


Figure 8. Comparison between the numerical result (---) and the experimental data (—) for the third test case.

ACKNOWLEDGMENT

This research was supported by Nelson Industries, Inc.

REFERENCES

1. T. W. WU and G. C. WAN 1996 *Journal of Vibration and Acoustics, ASME Transactions* **118**, 479–484. Muffler performance studies using a direct mixed-body boundary element method and a three-point method for evaluating transmission loss.
2. G. C. WAN 1995 *Proceedings of the 1995 International Conference on Noise Control Engineering*, 421–424. Prediction and measurement of the acoustic performance of mufflers.
3. J. IGARASHI and M. TOYAMA 1959 *Report No. 339, Aeronautical Research Institute, University of Tokyo*, Fundamentals of acoustical silencers (I)—theory and experiments of acoustic low-pass filters.
4. T. W. WU, P. ZHANG and C. Y. R. CHENG 1998 *Journal of Sound and Vibration* **217**, 767–779. Boundary element analysis of mufflers with an improved method for deriving the four-pole parameters.
5. J. KIM and W. SOEDEL 1989 *Journal of Sound and Vibration* **129**, 237–254. General formulation of four pole parameters for three dimensional cavities utilizing modal expansion with special attention to the annular cylinder.
6. J. KIM and W. SOEDEL 1989 *Journal of Sound and Vibration* **131**, 103–114. Analysis of gas pulsations in multiply connected three dimensional acoustic cavity with special attention to natural mode or wave cancellation effects.
7. J. KIM and W. SOEDEL 1990 *Journal of Vibration and Acoustics, ASME Transactions* **112**, 425–459. Development of general procedure to formulate four pole parameters by modal expansion and its application to three dimensional cavities.
8. Z. JI, Q. MA and Z. ZHANG 1994 *Journal of Sound and Vibration* **173**, 57–71. Application of the boundary element method to predicting acoustic performance of expansion chamber mufflers with mean flow.
9. A. FRID 1989 *Journal of Sound and Vibration* **133**, 423–438. Fluid vibration in piping systems—a structural mechanics approach, I: theory.

10. W. EVERSMAN 1987 *Transactions of the American Society of Mechanical Engineers Journal of Vibrations, Acoustics, Stress and Reliability in Design* **109**, 168–177. A systematic procedure for the analysis of multiply branched acoustic transmission lines.
11. R. GLAV and M. ABOM 1997 *Journal of Sound and Vibration* **202**, 739–747. A general formalism for analyzing acoustic 2-port networks.
12. T. TANAKA, T. FUJIKAWA, T. ABE and H. UTSUNO 1985 *Journal of Vibration, Acoustics, Stress, and Reliability in Design, ASME Transactions* **107**, 86–91. A method for the analytical prediction of insertion loss of a two-dimensional muffler model based on the transfer matrix derived from the boundary element method.
13. J. W. SULLIVAN and M. J. CROCKER 1978 *Journal of Acoustical Society of America* **64**, 207–215. Analysis of concentric-tube resonators having unpartitioned cavities.
14. A. PIERCE 1989 *Acoustics An Introduction to Its Physical Principles and Applications*. New York: Acoustical Society of America.